RSC Advances

PAPER

View Article Online
View Journal | View Issue

Cite this: *RSC Adv.*, 2017, **7**, 15817

A cancer cell-specific two-photon fluorescent probe for imaging hydrogen sulfide in living cells†

Xuezhen Song, Baoli Dong, Xiuqi Kong, Chao Wang, Nan Zhang and Weiying Lin*

Received 5th February 2017
Accepted 2nd March 2017

DOI: 10.1039/c7ra01479a

rsc.li/rsc-advances

Hydrogen sulfide (H_2S) could induce the proliferation of cancer cells in a concentration-dependent manner, and has close relation with the tumor growth. Monitoring the H_2S level in real-time is of great important for understanding its roles in the cancer cell proliferation and the diagnosis of the tumor. Herein, a novel cancer cell-specific two-photon fluorescent probe **BN-H_2S** for detecting H_2S in cancer cells was designed and synthesized. Biotin was selected as the cancer cell-specific group and the azide group was employed as the response site for H_2S. When **BN-H_2S** responded to H_2S, a turn-on fluorescence at 544 nm was observed clearly. **BN-H_2S** exhibited high selectivity for H_2S over other relative species. Under the guidance of the biotin group, **BN-H_2S** can be successfully used for the two-photon imaging of H_2S in cancer cells, while **BN-H_2S** showed relatively weak response for H_2S in normal cells. We expect that this design concept can be further developed for selectively detecting other biomolecules in living cancer cells.

1. Introduction

Hydrogen sulfide (H_2S) is a crucial gasotransmitter besides nitric oxide and carbon monoxide.[1,2] At normal levels, H_2S plays important roles in many physiological processes, such as relaxation of vascular smooth muscles,[3–5] inhibition of insulin signaling,[6] mediation of neurotransmission,[7–10] and suppress inflammation against oxidative stress.[11,12] Recent studies indicate that H_2S affects the proliferation of cancer cell in a concentration-dependent manner, and has closely relation with the cancer cell growth.[13,14] For example, Cao *et al.* demonstrated that H_2S could be endogenously produced in colon cancer cells (WiDr), and the exogenous H_2S at physiologically relevant concentrations could reduce the cell viability.[13] These studies suggest that H_2S is a proliferative factor in human colon cancer cells, and can lead to an in-depth understanding of cancer development. Therefore, monitoring H_2S level in real-time is of great important for the further understanding of its roles in the cancer cell proliferation, and also could provide novel H_2S-based strategy for the cancer therapy.

Traditionally, the most widely applied methods for detecting H_2S are methylene blue method,[15] the electrode method[16] and the monobromobimane method,[17,18] but these methods need destructive sampling and have limitation for the real-time detection of H_2S in living cells or tissues. Fluorescence imaging is a more attractive approach for detecting H_2S because of its numerous advantages, such as imperial spatiotemporal resolution, non-destructive testing and real-time detection.[19–21] So far, many fluorescent probes for H_2S have been reported.[22,23] However, to the best of our knowledge, these fluorescent probes all had no cancer cell-specific group and cannot distinguish cancer cells from normal cells. In addition, the two-photon imaging utilizes the long-wavelength light as excitation source, and generally has numerous advantages relative to one-photon imaging, such as reduced photodamage to biosamples and negligible background fluorescence.[24,25] Therefore, the construction of cancer cell-specific two-photon fluorescent probe for imaging H_2S in living system is still in demand.

In this work, we report a novel cancer cell-specific two-photon fluorescent probe (**BN-H_2S**) for detecting H_2S. In this probe, biotin was selected as the cancer cell-specific group, because the receptors related to the uptake of biotin are generally overexpressed on the cancer cell surface. Accordingly, **BN-H_2S** could discriminate the cancer cells from normal cells under the guidance of biotin group. The probe **BN-H_2S** has excellent sensitivity and selectivity for detecting H_2S. The bioimaging experiments demonstrate that **BN-H_2S** could be applied for the two-photon fluorescence imaging of H_2S in living cancer cells.

2. Experimental

2.1 Materials and instruments

All chemical reagents were commercial. Twice-distilled water was used in all the experiments. Thin Layer Chromatography (TLC) analysis was performed on the silica gel plates and the chromatography was performed using silica gel (mesh 200–300, Qingdao Ocean Chemicals). NMR spectra were obtained on an AVANCE III 400 MHz Digital NMR Spectrometer, and

Institute of Fluorescent Probes for Biological Imaging, School of Chemistry and Chemical Engineering, School of Materials Science and Engineering, University of Jinan, Jinan, Shandong 250022, P. R. China. E-mail: weiyinglin2013@163.com

† Electronic supplementary information (ESI) available: Supplementary spectra, NMR and HRMS data. See DOI: 10.1039/c7ra01479a

tetramethylsilane (TMS) was used as internal reference. High-resolution electronspray mass spectra (HRMS) were obtained from a Bruker APEX IV-FTMS 7.0T mass spectrometer. pH values were determined on a Mettler-Toledo Delta 320 pH meter. UV-vis absorption spectra were measured on a Shimadzu UV-2600 spectrophotometer. Fluorescence spectra were obtained with a Hitachi F4600 fluorescence spectrophotometer. HeLa cells, NIH 3T3 cells and calf bovine serum were obtained from the College of Life Science, Nankai University (Tianjin, China).

2.2 Synthesis of compound 2

Compound **1** was synthesized according to the previous report.[26] A mixture of compound **1** (636 mg, 2 mmol), biotin (488.62 mg, 2 mmol), EDCl (576 mg, 3 mmol), HOBt (675 g, 5 mmol) and DIEA (1 mL) in DMF (3 mL) was stirred for 12 h at room temperature. Then 6 mL water was added into the mixture and extracted with CH_2Cl_2, washed three times with water, dried over Na_2SO_4 and evaporated under reduced pressure to provide crude compound **2**. Then the crude product was purified by silica column chromatography (CH_2Cl_2 : MeOH = 10 : 1) to afford compound **2** (380 mg, yield 35%). ^{1}H NMR (DMSO-d_6, 400 MHz): δ 8.54–8.57 (m, 2H), 8.33–8.35 (d, J = 8.0 Hz, 1H), 8.22–8.24 (d, J = 8.0 Hz, 1H), 8.01–8.03 (t, 1H), 7.91–7.99 (t, 1H), 6.38–6.42 (d, J = 20.0 Hz, 2H), 4.29–4.32 (m, 1H) 4.11–4.14 (t, 2H), 4.04–4.07 (m, 1H), 2.94–2.99 (m, 1H), 2.78–2.82 (m, 1H), 2.56–2.59 (m, 1H), 1.91–1.94 (m, 2H), 1.55–1.56 (m, 1H), 1.38–1.40 (m, 3H), 1.19–1.21 (m, 3H). ^{13}C NMR (DMSO-d_6, 100 MHz): 172.77, 163.60, 163.55, 163.15, 132.96, 131.96, 131.82, 131.35, 130.29, 129.42, 129.29, 128.95, 123.48, 122.71, 61.43, 59.66, 55.81, 36.68, 35.69, 28.55, 28.44, 25.61. HRMS (ESI): m/z calculated for $C_{24}H_{25}BrN_4O_5S$ $[M + H]^+$ 545.0780, found: 545.0826.

2.3 Synthesis of BN-H_2S

Compound **2** (272 mg, 0.5 mmol), NaN_3 (65 mg, 1 mmol) were mixed in DMF (5.0 mL) and stirred at 50 °C for 4 h. Then 5 mL water was added into the mixture and extracted with CH_2Cl_2, washed three times with water, dried over Na_2SO_4 and evaporated under reduced pressure. The crude product was purified by silica column chromatography (CH_2Cl_2 : MeOH = 5 : 1) to afford **BN-H_2S** (147 mg, yield 58%) as an orange-yellow solid. ^{1}H NMR (DMSO-d_6, 400 MHz): δ 8.56–8.59 (m, 1H), 8.43–8.48 (m, 1H), 8.23–8.36 (m, 1H), 7.84–8.04 (m, 2H), 7.27–7.38 (m, 1H), 6.38–6.42 (d, J = 20.0 Hz, 2H), 4.29–4.32 (t, 1H), 4.11–4.14 (t, 2H), 4.05–4.06 (s, 1H), 2.97–2.99 (t, 1H), 2.78–2.82 (m, 1H), 1.91–1.94 (m, 2H), 1.48–1.53 (m, 1H), 1.35–1.39 (m, 3H), 1.18–1.24 (m, 4H), 0.82–0.87 (m, 1H). ^{13}C NMR (DMSO-d_6, 100 MHz): 172.65, 164.48, 163.58, 163.20, 153.10, 134.32, 131.38, 130.28, 129.72, 124.39, 122.41, 119.82, 108.53, 108.15, 61.40, 59.66, 55.81, 36.98, 35.72, 34.64, 28.53, 28.41, 25.62. HRMS (ESI): m/z calculated for $C_{24}H_{25}N_7O_4S$ $[M + H]^+$ 508.1761, found 508.1758.

2.4 Synthesis of BN-NH_2

The mixture of **BN-H_2S** (51 mg, 0.1 mmol) and Na_2S (39 mg, 0.5 mmol) in 2 mL DMF was stirred to room temperature for 6 h. Then 5 mL water was added into the mixture and extracted with CH_2Cl_2, washed three times with water, dried over Na_2SO_4 and evaporated under reduced pressure. The solid residue was purified by flash chromatography column using methanol/dichloromethane (v/v 1 : 10) to afford a yellow solid as **BN-NH_2** (36 mg, yield 75%). ^{1}H NMR (DMSO-d_6, 400 MHz): δ 8.61–8.63 (d, 1H), 8.42–8.44 (d, 1H), 8.18–8.20 (d, 1H), 7.87–7.90 (t, 1H), 7.64–7.68 (t, 1H), 7.45 (s, 2H), 6.83–6.85 (d, J = 8.0 Hz, 1H), 6.38–6.43 (d, J = 20.0 Hz, 2H), 4.29–4.32 (t, 1H), 4.03–4.12 (m, 3H), 2.95–2.99 (m, 1H), 2.78–2.82 (m, 1H), 2.58 (s, 1H), 1.93–1.97 (t, 2H), 1.50–1.53 (m, 1H), 1.38–1.44 (m, 3H), 1.19–1.22 (m, 3H), 0.82–0.87 (m, 1H). ^{13}C NMR (DMSO-d_6, 100 MHz): 172.74, 163.93, 163.56, 163.17, 143.18, 132.98, 131.97, 131.37, 128.93, 127.77, 124.00, 122.84, 118.86, 116.40, 63.43, 59.65, 55.82, 36.73, 35.69, 30.23, 29.10, 23.46, 23.09. HRMS (ESI): m/z calculated for $C_{24}H_{27}N_5O_4S$ $[M + H]^+$ 482.1857, found 482.1861; $[M + Na]^+$ 504.1681, found 504.1675.

2.5 Determination of fluorescence quantum yield

Fluorescence quantum yields were determined using Rhodamine-6G as reference (Φ_f = 0.94 in ethanol). The quantum yields were calculated following the equation: $\Phi_S = \Phi_R \times (I_S/I_R) \times (A_R/A_S) \times (\eta_S/\eta_R)^2$. Here, Φ_S and Φ_R are the quantum yields of sample and reference, I_S and I_R are the integrated emission intensities of the corrected spectra for the sample and reference, A_R and A_S stand for the absorbance of the reference and sample at the excitation wavelength, η_S/η_R are the values of refractive index for the respective solvent used for the sample and reference.

2.6 Measurements of two-photon cross section

Two-photon cross sections (δ) for **BN-H_2S** in absence and presence of Na_2S in PBS (20 mM, pH = 7.4, 5% MeOH) were determined following the previously reported methods, and Rhodamine 6G was selected as the reference.[27] The two-photon absorption cross section (δ) was calculated using the equation: $\delta = \delta_r(S_s\Phi_r\phi_r c_r)/(S_r\Phi_s\phi_s c_s)$, where the subscripts s and r stand for the sample and reference molecule, S is the intensity of the signal collected using a CCD detector. Φ is the fluorescence quantum yield, and ϕ stands for the overall fluorescence collection efficiency of the experimental apparatus. c is the concentration, and δ_r is the two-photon absorption cross section of Rhodamine 6G.

2.7 Cytotoxicity experiments

Cytotoxic effects of **BN-H_2S** were evaluated using the MTT assay. HeLa and NIH 3T3 cells were seeded into 96 well-plates at the density of 3000 cells per well. After 24 h of cell attachment, various concentrations of **BN-H_2S** were added into wells for the further cultured of 24 h. Then, 10 μL of MTT (5 μg mL^{-1}) were mixed into cells for incubated another 4 h. After that, 100 μL of DMSO were used to resolve the formazan. The plate was shaken for 20 min, and then the absorbance was determined at 570 nm by a microplate reader (Thermo Fisher Scientific). Cell viability was expressed as a percentage of the control culture value.

2.8 Cell culture and fluorescence imaging

HeLa and NIH 3T3 cells were cultured in modified Eagle's medium supplemented with 10% calf bovine serum in an atmosphere of 5% CO_2 and 95% air at 37 °C. The cells were seeded into the glass-bottom culture dishes and cultured for 24 h. For the imaging of Na_2S, the cells were incubated with 10 μM **BN-H_2S** for 15 min at 37 °C, then the media was replaced with PBS. The cells were then incubated with Na_2S for another 30 min, and then the imaging was performed using a Nikon A1R MP+ confocal microscope.

3. Results and discussion

3.1 Design and synthesis of BN-H_2S

As shown in Scheme 1, the designed probe **BN-H_2S** was made of three factors including cancer cell-specific group, two-photon fluorophore and H_2S response site. Initially, biotin was selected as the cancer cell-specific group, because the receptors related to the uptake of biotin are generally overexpressed on the cancer cell surface to sustain the rapid growth of the cancer cells, and the biotin can be chemically modified easily. Previously, many studies also demonstrated that biotin could be used as a cancer-targeting molecule.[28,29] Naphthalimide fluorophore was employed as the two-photon fluorophore due to its significant advantages in optical properties, including excellent photostability, high fluorescence quantum yield and desirable two-photon emission properties. In addition, the azide group was employed as the response site because of its highly selective and sensitive response for H_2S. With these considerations in mind, we constructed a biotin-guided two-photon fluorescent probe **BN-H_2S** for detecting H_2S. **NA-H_2S** has no biotin group was selected as the control compound, and was synthesized according to the previous report.[30] The synthesis route of **BN-H_2S** was shown in Scheme 1, and the structure was determined by HRMS, ^{1}H NMR and ^{13}C NMR spectra (ESI†).

3.2 Optical response of BN-H_2S to H_2S

Initially, we determined the optical response of **BN-H_2S** to H_2S in PBS (20 mM, pH = 7.4, 5% MeOH) using UV-vis absorption spectra. Na_2S was selected as H_2S source. As shown in Fig. 1, **BN-H_2S** exhibited a main absorption maximum at 366 nm with molar absorption coefficient (ε) of 0.77 × 10^4 M^{-1} cm^{-1} arised from the naphthalimide fluorophore. Upon the addition of Na_2S, the absorbance at 366 nm decreased and a new absorption at 432 nm appeared, indicating that the reaction between **BN-H_2S** and H_2S indeed occurred.

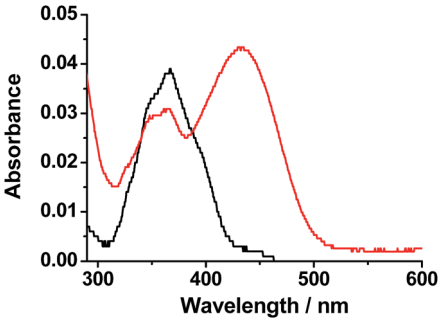

Fig. 1 Absorption spectra of 5 μM BN-H_2S in absence (black) and presence (red) of 100 μM Na_2S in PBS (20 mM, pH = 7.4, 5% MeOH).

Subsequently, the optical response of **BN-H_2S** to H_2S in PBS was investigated using fluorescence spectra. As shown in Fig. 2, **BN-H_2S** itself showed weak fluorescence under the excitation at 440 nm with the fluorescence quantum yield (Φ) of 0.01. Upon the addition Na_2S, the fluorescence intensity at 544 nm increased gradually with raising the Na_2S concentration, corresponding to the fluorescent color of **BN-H_2S** solution changed from weak green to strong green after the addition of Na_2S under the irradiation of 365 nm ultraviolet light. An excellent linearity between the fluorescence intensity at 544 nm and Na_2S concentration in the range of 0–80 μM was observed, and the detection limit was calculated to 71 nM (S/N = 3) according to IUPAC recommendations. Therefore, **BN-H_2S** has highly sensitivity and can potentially be applied for detecting H_2S in living system.

The response mechanism of **BN-H_2S** to H_2S was further explored on the basis of the HRMS data and the reaction experiment of **BN-H_2S** and Na_2S. The azide group can be liable to be reduced to amino by H_2S chemically, and the response

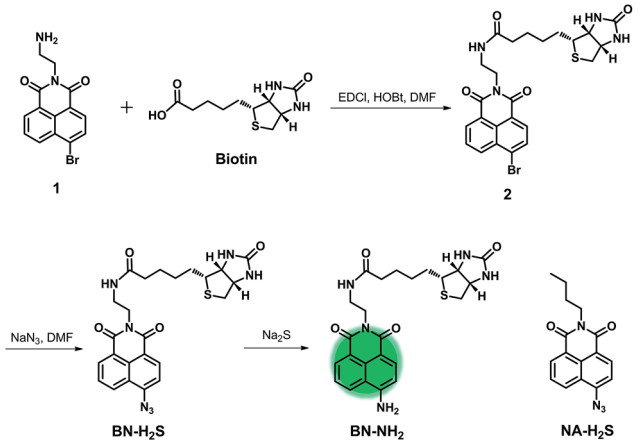

Scheme 1 Synthesis route of BN-H_2S and chemical structure of NA-H_2S.

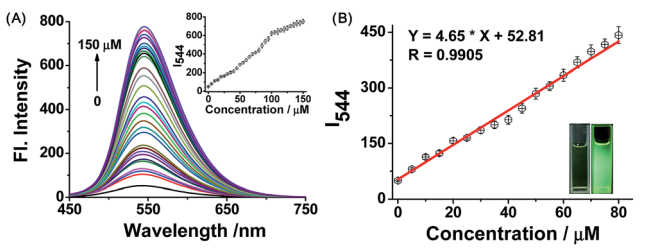

Fig. 2 (A) Fluorescence spectra of 5 μM BN-H_2S upon the addition of 0–150 μM Na_2S in PBS (20 mM, pH = 7.4, 5% MeOH) with the excitation at 440 nm, inset: the fluorescence intensity at 544 nm as a function of Na_2S concentration. (B) Linearity between the fluorescence intensity at 544 nm and Na_2S concentration in the range of 0–80 μM, inset: images of 5 μM BN-H_2S in absence (left) and presence (right) of 100 μM Na_2S under a UV lamp at 365 nm.

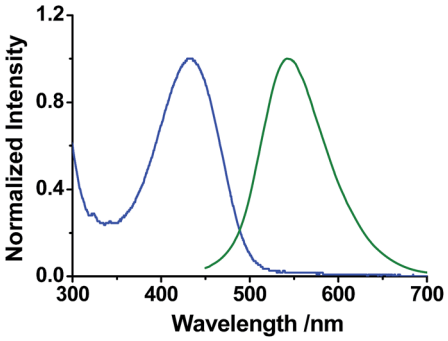

Fig. 3 Normalized absorption (blue) and fluorescence spectra (green, λ_{ex} = 440 nm) of 5 μM **BN-NH$_2$** in PBS (pH 7.4, 20 mM, 5% MeOH).

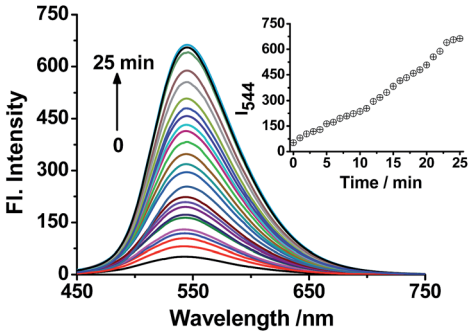

Fig. 5 Time-dependent fluorescence spectra of 5 μM **BN-H$_2$S** upon addition of 100 μM Na_2S in PBS (20 mM, pH = 7.4, 5% MeOH) with the excitation at 440 nm, inset: fluorescence intensity at 544 nm as a function of time.

mechanism of **BN-H$_2$S** to H_2S was proposed to be based on the reduction of nitrine (Scheme S1†). As shown in the HRMS assay (Fig. S1†), the two peaks at 482.1861 and 504.1671 corresponding to **BN-NH$_2$** (calcd $[M + H]^+$, 482.1857 and $[M + Na]^+$, 504.1681) were clearly observed, indicating that **BN-H$_2$S** can be reduced to **BN-NH$_2$** in PBS. Meanwhile, **BN-H$_2$S** can react with Na_2S in DMF for 6 h, to afford the product **BN-NH$_2$** with a yield of 75% (Scheme 1). **BN-NH$_2$** displayed the main absorption at 432 nm and fluorescence at 544 nm (Φ = 0.29) under excitation at 440 nm in PBS, consisting well with the absorption and fluorescence spectra of **BN-H$_2$S** after responding to Na_2S (Fig. 3). Therefore, the response mechanism of **BN-H$_2$S** to H_2S was proposed to base on the reduction of azide group.

The selectivity of **BN-H$_2$S** to H_2S was evaluated by determining the fluorescence spectra of **BN-H$_2$S** with various biologically relevant species in PBS (pH 7.4, 20 mM, 5% MeOH). We selected a serious of small biomolecules and ions that commonly exist in living systems as potential competitive analytes, such as Cys, GSH, SO_3^{2-}, H_2O_2. After the addition of Na_2S, the absorption at 432 nm appeared obviously, while the absorption spectra of **BN-H$_2$S** had no marked change upon the addition of other relevant species (Fig. S2†). As shown in Fig. 4, only Na_2S can trigger a significantly enhanced fluorescence at 544 nm, while the other relevant species showed no marked influence on the fluorescence spectra of **BN-H$_2$S**. It indicates that **BN-H$_2$S** has excellent selectivity for H_2S and can be potentially used for detecting H_2S in living system.

Time-dependent fluorescence spectra of **BN-H$_2$S** in the presence of Na_2S were studied. Upon the addition of 100 μM Na_2S to **BN-H$_2$S** solution, the fluorescence intensity at 544 nm increased gradually with time, and reached the maximum within 25 min (Fig. 5). It indicates that the probe **BN-H$_2$S** could show response to H_2S in a short time. In addition, **BN-H$_2$S** displayed very weak fluorescence in the pH range of 4.0–10.0 (Fig. S3†). Upon the addition of Na_2S, the enhanced fluorescence at 544 nm was observed clearly. However, the fluorescence response of **BN-H$_2$S** to Na_2S tended to occur at weak basic condition, probably because the H_2S (pK_{a1} = 6.88) could be ionized to HS^- at weak basic condition, which has stronger nucleophilicity relative to H_2S and benefits for the reduction of azide group. Considering the physiological pH of 7.4 and the desirable response of **BN-H$_2$S** to H_2S at this pH, **BN-H$_2$S** can be potentially used for detecting H_2S in living system.

Furthermore, the two-photon properties of **BN-H$_2$S** in absence and presence of Na_2S were investigated by determining its two-photon action spectra ($\delta\Phi$). As shown in Fig. 6, **BN-H$_2$S** displayed nearly no two-photon property, while it displayed the maximum $\delta\Phi$ values of about 82 GM after the treatment of Na_2S. It indicates that **BN-H$_2$S** could be potentially served as a two-photon probe for determining H_2S in living systems.

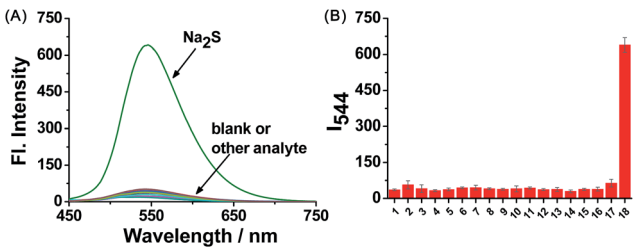

Fig. 4 Fluorescence spectra (A) and fluorescence intensity at 544 nm (B) of 5 μM **BN-H$_2$S** to various species in PBS (pH 7.4, 20 mM, 5% MeOH) under excitation at 440 nm. 1, blank; 2, GSH; 3, Cys; 4, Hcy; 5, $FeCl_2$; 6, VC; 7, NaF; 8, NaBr; 9, NaI; 10, $NaNO_2$; 11, H_2O_2; 12, NaClO; 13, $^{\bullet}OH$; 14, $MgCl_2$; 15, $ZnCl_2$; 16, NO; 17, Na_2SO_3; 18, Na_2S. Concentration: Cys and GSH, 1 mM; the other species, 100 μM.

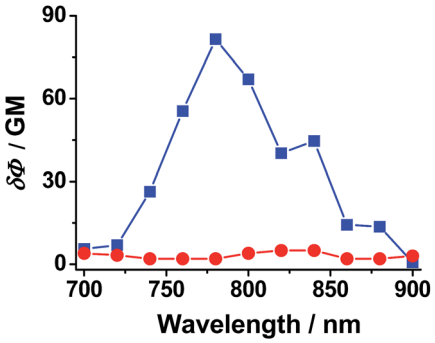

Fig. 6 Two-photon action ($\delta\Phi$) spectra of **BN-H$_2$S** in absence (red) and presence (blue) of Na_2S in PBS (20 mM, pH = 7.4, 5% MeOH).

3.3 Fluorescence imaging of BN-H_2S in living cells

To confirm the cancer cell-specific capacity of **BN-H_2S** and the two-photon fluorescence response of **BN-H_2S** to H_2S, the fluorescence imaging experiments were performed in cancer and normal cells, respectively. In consideration of the different expression quantities of biotin receptor on the cell surface, HeLa and NIH 3T3 cells were selected as cancer and normal cell models, respectively. MTT assays indicate that **BN-H_2S** had no marked cytotoxicity for HeLa and NIH 3T3 cells at the concentration of 10 μM (Fig. S4†), and could be suitable for the cell imaging. HeLa and NIH 3T3 cells were incubated with 10 μM **BN-H_2S** for 20 min, and then the cells were incubated with Na_2S for another 15 min. As shown in Fig. 7, the HeLa cells treated with only **BN-H_2S** showed nearly no fluorescence, and displayed strong green fluorescence after the further incubation with Na_2S under the one-photon or two-photon excitation. However, when pretreated with 2 mM biotin and further incubated with **BN-H_2S** and Na_2S, HeLa cells showed relatively weak fluorescence under the one-photon or two-photon excitation, indicating the biotin can bond to the receptor and then adverse to the cell uptake of **BN-H_2S**. Meanwhile, compared with HeLa cells, NIH 3T3 cells had weak green fluorescence when treated with **BN-H_2S** and Na_2S (Fig. 8). It indicates that the **BN-H_2S** has higher affinity for the HeLa cells, likely because of the higher expression quantity of biotin receptor on the HeLa cell surface relative to NIH 3T3 cell surface. As the control experiments, the **NA-H_2S** which has no biotin group, can be applied for the imaging of H_2S in both HeLa and NIH 3T3 cells (Fig. S5†). Moreover, under two-photon excitation at 760 nm, the fluorescence peaks at about 540 nm were observed when **BN-H_2S** responded H_2S in PBS, HeLa cells and 3T3 cells, further confirming that the detectable fluorescence in cells can be ascribed to the response of **BN-H_2S** to H_2S (Fig. 9). To the best of our knowledge, the cancer cell-specific two-photon probe **BN-H_2S** for monitoring H_2S in living cells was reported for the first time. Taken together, the **BN-H_2S** can be used as a cancer cell-specific two-photon probe for detecting H_2S in living cells.

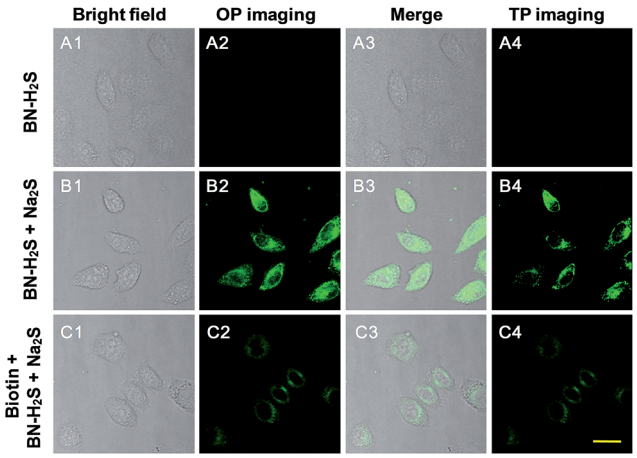

Fig. 7 (A) Fluorescence images of HeLa cells treated with 10 μM BN-H_2S; (B) fluorescence images of HeLa cells treated with 10 μM BN-H_2S and 100 μM Na_2S; (C) fluorescence images of HeLa cells pretreated 2 mM biotin and further treated with 10 μM BN-H_2S and 100 μM Na_2S. One-photon (OP) imaging: emission at 500–550 nm with excitation at 488 nm; two-photon (TP) imaging: emission at 500–550 nm with excitation at 760 nm. Scale bar = 20 μm.

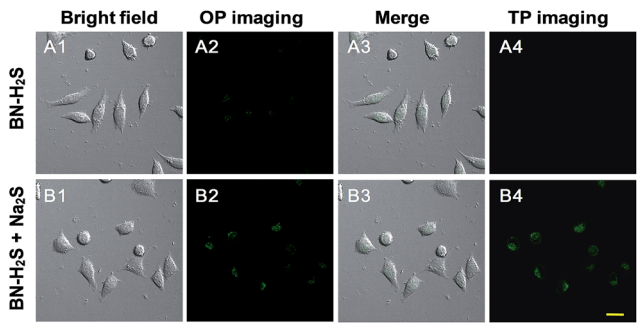

Fig. 8 (A) Fluorescence images of NIH 3T3 cells treated with 10 μM BN-H_2S. (B) Fluorescence images of NIH 3T3 cells treated with 10 μM BN-H_2S and 100 μM Na_2S. One-photon (OP) imaging: emission at 500–550 nm with excitation at 488 nm; two-photon (TP) imaging: emission at 500–550 nm with excitation at 760 nm. Scale bar = 20 μm.

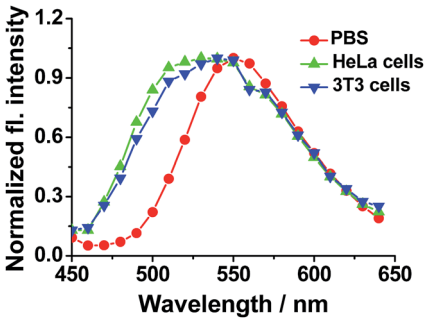

Fig. 9 Normalized two-photon fluorescence spectra (λ_{ex} = 760 nm) of 10 μM BN-H_2S in presence of 100 μM Na_2S in PBS (20 mM, pH = 7.4, 5% MeOH), HeLa cells and 3T3 cells, respectively.

4. Conclusions

In conclusion, we have designed a novel cancer cell-specific two-photon fluorescent probe **BN-H_2S** for detecting H_2S in cancer cells. In **BN-H_2S**, biotin was selected as the cancer cell-specific group and the azide group was employed as the response site. When **BN-H_2S** responded to H_2S, the azide group was fast reduced to amide, and the turn-on green fluorescence was observed obviously. The probe exhibited excellent sensitivity with the detection limit of 71 nM, and high selectivity for H_2S over the other relative species. Under the guidance of biotin group, **BN-H_2S** can be successfully applied for the two-photon imaging of H_2S in living cancer cells. We expect that this design concept could be further developed for the detection of other biomolecules in the living cancer cells.

Acknowledgements

This work was financially supported by NSFC (21472067, 21672083, 51602127), Taishan Scholar Foundation (TS 201511041), and the startup fund of the University of Jinan (309-10004).

References

1 R. Wang, *Antioxid. Redox Signaling*, 2010, **12**, 1061–1064.
2 K. Shimamoto and K. Hanaoka, *Nitric Oxide*, 2015, **46**, 72–79.
3 G. D. Yang, L. Y. Wu, B. Jiang, W. Yang, J. S. Qi, K. Cao, Q. Meng, A. K. Mustafa, W. Mu, S. Zhang, S. H. Snyder and R. Wang, *Science*, 2008, **322**, 587–590.
4 B. D. Paul and S. H. Snyder, *Nat. Rev. Mol. Cell Biol.*, 2012, **13**, 499–507.
5 J. W. Elrod, J. W. Calvert, J. Morrison, J. E. Doeller, D. W. Kraus, L. Tao, X. Jiao, R. Scalia, L. Kiss, C. Szabo, H. Kimura, C. W. Chow and D. J. Lefer, *Proc. Natl. Acad. Sci. U. S. A.*, 2007, **104**, 15560–15565.
6 Y. Kaneko, Y. Kimura, H. Kimura and I. Niki, *Diabetes*, 2006, **55**, 1391–1397.
7 K. Eto, T. Asada, K. Arima, T. Makifuchi and H. Kimura, *Biochem. Biophys. Res. Commun.*, 2002, **293**, 1485–1488.
8 K. Abe and H. Kimura, *J. Neurosci.*, 1996, **16**, 1066–1071.
9 H. Kimura, *Neurochem. Int.*, 2013, **63**, 492–497.
10 K. Fukami, F. Sekiguchi, M. Yasukawa, E. Asano, R. Kasamatsu and M. Ueda, *Biochem. Pharmacol.*, 2015, **97**, 300–309.
11 L. Li, M. Bhatia, Y. Z. Zhu, Y. C. Zhu, R. D. Ramnath, Z. J. Wang, F. B. Mohammed Anuar, M. Whiteman, M. Salto-Tellez and P. K. Moore, *FASEB J.*, 2005, **19**, 1196–1198.
12 M. L. Lo Faro, B. Fox, J. L. Whatmore, P. G. Winyard and M. Whiteman, *Nitric Oxide*, 2014, **41**, 38–47.
13 Q. Cao, L. Zhang, G. Yang, C. Xu and R. Wang, *Antioxid. Redox Signaling*, 2010, **12**, 1101–1109.
14 W. J. Cai, M. J. Wang, L. H. Ju, C. Wang and Y. C. Zhu, *Cell Biol. Int.*, 2010, **34**, 565–572.
15 V. Kuban, P. K. Dasgupta and J. N. Marx, *Anal. Chem.*, 1992, **64**, 36–43.
16 D. M. Tsai, A. S. Kumar and J. M. Zen, *Anal. Chim. Acta*, 2006, **556**, 145–150.
17 C. M. Klingerman, N. Trushin, B. Prokopczyk and P. Haouzi, *Am. J. Physiol.*, 2013, **305**, 630–638.
18 M. Nishida, T. Sawa, N. Kitajima, K. Ono, H. Inoue, H. Ihara, H. Motohashi, M. Yamamoto, M. Suematsu, H. Kurose, A. Vliet, B. Freeman, T. Shibata, K. Uchida, Y. Kumagai and T. Akaike, *Nat. Chem. Biol.*, 2012, **8**, 714–724.
19 J. R. Lakowicz, *Principles of Fluorescence Spectroscopy*, Springer, New York, 3rd edn, 2006.
20 Y. Kushida, T. Nagano and K. Hanaoka, *Analyst*, 2015, **140**, 685–695.
21 B. Dong, X. Song, X. Kong, C. Wang, Y. Tang, Y. Liu and W. Lin, *Adv. Mater.*, 2016, **28**, 8755–8759.
22 V. S. Lin, W. Chen, M. Xian and C. J. Chang, *Chem. Soc. Rev.*, 2015, **44**, 4596–4618.
23 X. Li, X. Gao, W. Shi and H. Ma, *Chem. Rev.*, 2014, **114**, 590–659.
24 L. Qian, L. Liand and S. Q. Yao, *Acc. Chem. Res.*, 2016, **49**, 626–634.
25 K. Zheng, W. Lin, L. Tan, H. Chen and H. Cui, *Chem. Sci.*, 2014, **5**, 3439–3448.
26 X. Zhou, F. Su, H. Lu, P. Senechal-Willis, Y. Tian, R. H. Johnson and D. R. Meldrum, *Biomaterials*, 2012, **33**, 171–180.
27 N. S. Makarov, M. Drobizhev and A. Rebane, *Opt. Express*, 2008, **6**, 4029–4047.
28 S. Chen, X. Zhao, J. Chen, J. Chen, L. Kuznetsova, S. S. Wong and I. Ojima, *Bioconjugate Chem.*, 2010, **12**, 979–987.
29 Y. H. Lee, Y. Tang, P. Verwilst, W. Lin and J. S. Kim, *Chem. Commun.*, 2016, **52**, 11247–11250.
30 L. Zhang, S. Li, M. Hong, Y. Xu, S. Wang, Y. Liu, Y. Qian and J. Zhao, *Org. Biomol. Chem.*, 2014, **12**, 5115–5125.